applied sciences

MDPI

Article

Source Apportionment of Atmospheric Aerosols in Kraków, Poland, before and during the COVID-19 Pandemic at a Traffic Monitoring Station

Lucyna Samek [1,*], Anna Ryś [1], Jan Dudek [1], Zdzisław Stęgowski [1], Vânia Martins [2], Susana Marta Almeida [2] and Katarzyna Styszko [3,*]

[1] Faculty of Physics and Applied Computer Science, AGH University of Krakow, Al. Mickiewicza 30, 30-059 Krakow, Poland; turekfijak@agh.edu.pl (A.R.); jand98@wp.pl (J.D.); zdzislaw.stegowski@fis.agh.edu.pl (Z.S.)
[2] Instituto Superior Técnico, Universidade de Lisboa, Centro de Ciências e Tecnologias Nucleares, Estrada Nacional 10, Km 139.7, 2695-066 Bobadela, Portugal; vania.martins@ctn.tecnico.ulisboa.pt (V.M.); smarta@ctn.tecnico.ulisboa.pt (S.M.A.)
[3] Faculty of Energy and Fuels, AGH University of Krakow, Al. Mickiewicza 30, 30-059 Krakow, Poland
* Correspondence: lucyna.samek@fis.agh.edu.pl (L.S.); styszko@agh.edu.pl (K.S.)

Abstract: PM_{10} samples were collected at the Kraków air quality traffic monitoring station during two periods: February–May 2018 and February–June 2020. The PM_{10} concentrations dropped by 50% from 74 ± 29 μg/m^3 to 37 ± 13 μg/m^3 in 2018 and 2020, respectively. The elemental concentrations were determined by the energy-dispersive X-ray fluorescence (EDXRF) method, and the ion concentrations were determined by ion chromatography (IC). The concentration ratios in 2018 to 2020 were greater than 1.7 for the following elements: S, Cl, K, Zn, Br, and the ions SO_4^{2-}, Na^+, and NH_4^+. Similar concentrations were observed in 2018 and 2020 for the following chemical species: Ca, Ti, Mn, Ni, Rb, Sr, K^+, Mg^{2+}, Ca^{2+}, and PO_4^{3-}. The Cr concentration was higher in 2020 compared to 2018. Four source profiles were obtained from the PMF (Positive Matrix Factorization) modelling. The following sources were attributed to this: solid fuel combustion, secondary inorganic aerosols, traffic/industry/construction work, and soil. The contributions of solid fuel combustion and secondary inorganic aerosols (SIA) were significantly lower in February and March 2020 than in February and March 2018. The relative differences were in the range 70–98%. Traffic/industry/construction work contributions were 6% and 36% lower in March and May 2020 compared to the same months in 2018, respectively. Two factors affected the characteristics of PM_{10}: one was the ban of using coal and wood for heating purposes introduced in Krakow in September 2019, observed mainly in February and March, and the COVID-19 pandemic that was observed mainly in April and May.

Keywords: PM_{10}; EDXRF; IC; PMF

Citation: Samek, L.; Ryś, A.; Dudek, J.; Stęgowski, Z.; Martins, V.; Almeida, S.M.; Styszko, K. Source Apportionment of Atmospheric Aerosols in Kraków, Poland, before and during the COVID-19 Pandemic at a Traffic Monitoring Station. *Appl. Sci.* **2023**, *13*, 11492. https://doi.org/10.3390/app132011492

Academic Editor: Fulvia Chiampo

Received: 31 August 2023
Revised: 8 October 2023
Accepted: 18 October 2023
Published: 20 October 2023

1. Introduction

Public awareness of the air quality around the world is increasing. Many actions are being taken to increase environmental awareness. Local authorities around the world make decisions to reduce the levels of air particulate matter (APM). The environmental protection agencies prepared regulations according to the limit values of chemical substances in the atmosphere. The regulation is applicable to the European Union in accordance with the Directive 2008/50/EC [1]. However, in many cities, these limit values are still exceeded [1–3]. The influence of particulate matter on human health and the environment requires knowledge of the chemical content and size distribution of APM. Many studies have researched the characterization of particulate matter [4–7]. Some of them also include the health effects of APM [8,9]. APM can cause cardiovascular and respiratory diseases

and cancer. APM is associated with millions of premature deaths worldwide and with cardiovascular and respiratory diseases every year [10–13]. Atmospheric PM varies in size and composition and consists of a mixture of primary pollutants (emitted directly from anthropogenic and natural sources) and secondary pollutants (formed in the atmosphere through reactions of primary pollutants) [14]. The chemical composition of particulate matter, as well as other characteristics of PM, can vary within wide limits in different areas, depending on the main emission sources, dispersion conditions, and chemical reactions that take place in the atmosphere, as well as the influence of the air masses transported from both neighboring and remote areas [14]. The contribution of sources is evaluated by different methods, such as receptor modelling. One such method is positive matrix factorization (PMF) [6,7,15,16]. In some papers, SA methods have been described [16–20]. The main sources of PM determined by receptor modelling (108 European SA analysis) are the following: sea salt, soil, traffic exhaust, traffic non-exhaust, industry, secondary inorganic aerosols, solid fuel combustion (biomass burning and coal combustion) and other non-identified sources [15,16]. A review of SA techniques conducted by Johnson et al. [21] identified 11 common PM source categories in 18 developing countries of Asia, Africa, and Latin America, grouped into four main types: (1) dust emissions, including road dust, soil dust, resuspension, fugitive dust, and construction; (2) transport (gasoline and diesel); (3) industrial activities, including coal and oil burning, brick kilns and power plants; as well as (4) nonurban, including biomass burning, long-range transport and marine sources. As a result, the chemistry, size distribution, or reactivity of PM vary widely from location to location and season to season, which induces large changes in health impacts depending on all of these parameters [22].

Krakow was one of the most polluted cities in Poland and Europe. Now, the situation is much better [23]; local authorities have taken many actions to reduce pollution in the city. In southern Poland, along the Vistula valley, the compact buildings and the location of Krakow in a concave form of land, isolated from the south by the mountain area, hinder the natural ventilation of the city via horizontal ventilation, i.e., the movement of pollutants by the emission wind from the place of emission to other areas [24,25]. The main sources in Krakow are road traffic, solid fuel combustion, and industry. The Arcellor Mittal steel industry is located in the east part of the city. The power plants (PGE Energia Cieplna S.A. and CEZ Skawina S.A.) are in the east and southwest parts of the city, respectively. Source apportionment and chemical characterization have been carried out in Krakow since 2014 [26–29]. PM_{10} was characterized in the summer of 2018 and winter 2018/2019 at urban and traffic background stations in Kraków [30]. For the use of PMF, five sources of particles have been identified for each station: fossil fuel combustion, secondary inorganic aerosols, traffic exhaust, soil, and the fifth source includes road dust, industry, and construction [30]. The study of Cassoto et al. [31] (2022) described the sources of organic aerosols of PM_{10} and PM_1 in 2018 in Krakow.

The first case in Europe of the transmission of severe acute respiratory syndrome coronavirus 2 (SARS-CoV-2), the virus that causes coronavirus disease 2019 (COVID-19), was detected on 20 February 2020 in Italy. In March, there was a large increase in the number of confirmed cases in many European countries, including Italy, Spain, Germany, and Great Britain. Lockdowns were imposed that led to a drastic reduction in the use of fossil fuels [32,33]. In Poland, the pandemic restrictions started on 11 January 2020. Some limitations in the activity of people were introduced step by step in March, April, and May 2020. An improvement in the air quality was observed during that time. PM_{10} was significantly lowered, especially at traffic monitoring stations. This could be due to decreased transport and anthropogenic activity during the COVID-19 pandemic.

The purpose of our research was to characterize PM_{10} and its sources in Krakow (Poland) for two periods of time. Prior to the COVID-19 epidemic and the introduction of a ban on individual heating with coal and wood in Kraków, sampling campaigns were carried out. The samples were collected in Spring 2018 and Spring 2020 at the Krakow

Traffic Monitoring Station. Positive matrix factorization was used for the source attribution study. The contributions of different sources were determined.

2. Materials and Methods

2.1. Sampling

PM_{10} samples were collected at the traffic monitoring station (Ave. Krasińskiego 50.057678; 19.926189) in Krakow during two periods: 2 February–30 May 2018 and 2 February–17 June 2020. The 24 h samples were collected on quartz filters by the Voivodeship Inspectorate for Environmental Protection and the Chief Inspectorate of Environmental Protection. This station is located between a three-lane dual carriageway. This road is one of the most congested streets in the city and is used by passenger cars and buses. Furthermore, the sampling location is about 1 km from the Old Town and 400 m from the Vistula River. The filter is stored in a refrigerator at +4 C. The samples from every third day were taken to the analyses. A total of 60 samples from both campaigns were selected for chemical analysis. Figure 1 presents a map with the location of the sampling site.

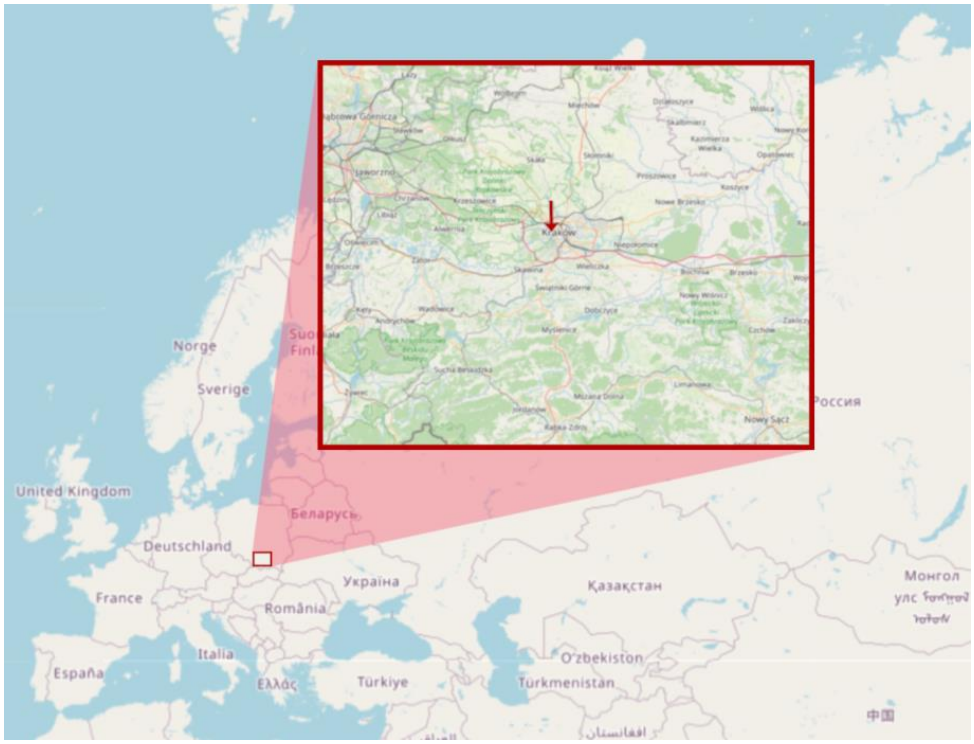

Figure 1. The map with the location of the sampling site (Av. Krasińskiego, traffic air monitoring station).

2.2. Elemental Analysis

The filters were weighed before and after sampling, following the PN-EN 12,341 standard procedure [34]. They were conditioned before weighing at a temperature of 20 ± 1 °C and constant relative humidity (50 ± 5%) for 48 h. The concentrations of the following elements were determined: P, S, Cl, K, Ca, Ti, V, Cr, Mn, Fe, Co, Ni, Zn, Cu, Br, Rb, Sr, As, and Pb. Energy-dispersive X-ray fluorescence (EDXRF) method was used for the quantification of elements' concentrations. Analysis was performed under the following conditions: 55 kV voltage, 30 mA current, and 2400 s measuring time. EDXRF spectrometer calibration was performed using thin film standards (Micromatter, Surrey, BC, Canada). The following standards were used for the calibration: SiO, KCl, CaF_2, ScF_3, Ti, V, Cr, Mn, Fe, Ni, CuS_x, ZnTe, Se, SrF_2, GaP, Ge, YF_3, ZrF_4, MoO_3, Ag, CsBr, TbF_3, Ba, WO_3, Au, and Pb. The calibration was verified by analyzing the U.S. NIST standard

SRM 2783 (Air Particulate Matter on Filter Media) [28,29]. Figure 2 shows the results of calibration validation.

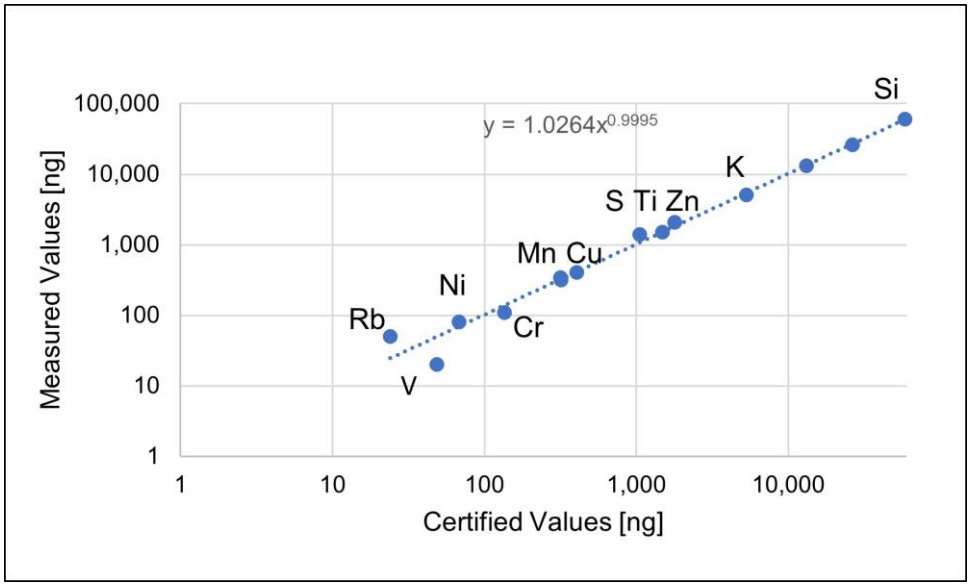

Figure 2. Validation of the calibration of EDXRF method by SRM 2783.

2.3. Ion Analysis

Isocratic ion chromatography on an ICS-1100 instrument (Thermo Scientific, Sunnyvale, CA, USA) equipped with an auto-sampler (AS-DV Thermo Scientific, Sunnyvale, USA) was used for the determination of the concentrations of ions (Na^+, K^+, Mg^{2+}, Ca^{2+}, NH_4^+, NO_3^-, Cl^-, PO_4^{3-}, and SO_4^{2-}). Separations were performed using an Ion Pac AS22 and analytical column CS16 for anions and cations, respectively. The separations of samples (25 µL injection volume) were performed with a flow rate of 1.2 mL min^{-1} of the mobile phase. Separated ion concentrations were determined after electrochemical suppression using AERS 500 and CERS 500 (Thermo Scientific, Sunnyvale, CA, USA) suppressors for anions and cations, respectively. Calibration was performed against external standards (Dionex Combined Seven Anion Standard II and Dionex Combined Six Cation Standard-II) diluted from stock solutions supplied by Thermo Scientific. The detection limits (DL) for selected ions were evaluated in triplicate analysis of standard deviation analysis for blank field samples and their minimum concentrations were detected in the ranges 0.05–0.14 µg/m^3 and 0.001–0.07 µg/m^3, for anions and cations, respectively. Details of the analytical procedure are presented elsewhere [27].

2.4. Elemental Enrichment Factors

An evaluation of element enrichment factors (EF) was carried out and the nature and human origin of elements were assessed. The EF was calculated using Belis and colleagues' formulas [15]:

$$EF = \frac{\frac{XPM}{RPM}}{\frac{XCrust}{RCrust}}, \quad (1)$$

where X PM and RPM are the concentrations of the element under consideration and the reference element in PM, respectively. XCrust and RCrust are the concentrations of the element under consideration and the reference element in the Earth's Crust, respectively. These measurements were taken from EDXRF measurements. PM and crust mean the concentrations in PM and in the Earth's crust. Three groups of sources are presented: (i) EF < 10 indicates the crustal origin of the element; (ii) 10 < EF < 100 indicates a mixed origin of the elements (natural and anthropogenic); and (iii) EF > 100 indicates an anthropogenic origin of a given element. EF calculations of EF were performed for Ti as a reference

element (if Ti is taken as a reference element EFTi = 1). The abundances of elements in the Earth's crust were taken from the publication by Rudnick et al. [35].

2.5. PMF Modelling

One of the methods that allows for the identification of particulate matter sources and the quantification of their contribution is the positive matrix factorization method (PMF) introduced by Paatero et al. [36] Due to the need to have many samples (at least several dozen), it is often classified as a statistical method. The basic assumption of the method is a constant relative share of components that characterize a given source. This share is called the profile of a given source. The PMF method, based on the matrix of the sample of chemical species of particulate matter, calculates the matrix of participation of a given number of factors and profiles of these factors [37]. The PMF receptor model solves the set of equations:

$$x_{ij} = \sum_{k=1}^{p} g_{ik} f_{kj} + e_{ij}, \quad (2)$$

where x_{ij} is an element of the concentration matrix X (i sample index and j species index), g_{ik} is an element of the contribution matrix G with p sources (k is the index of the sources), f_{kj} is an element of F the source and, finally, eij is an element of the residual matrix E [38]. The PMF multivariate statistical method decomposes the concentration matrix (X) into the source contribution (G) and source profile (F) matrixes in such a way that G and F obtain non-negative values only, ensuring the physical meaning of the model. The profile determines the share of individual components in each factor and is the basis for the physical assignment of a given factor to identify the sources of particulate matter. In this method, the number of factors is set arbitrarily. In practice, modeling is carried out for a different number of factors, and the number for which the determination of sources is unambiguous is finally selected [26]. In this work, the EPA PMF 5.0 software, developed by the US Environmental Protection Agency (US EPA), was used. As input, not only is the concentration matrix (X) required but also the appropriate uncertainty matrix (U). For a given number of factors (p), the matrixes G and F are adjusted by minimizing the objective function Q, which is defined as follows:

$$Q = \sum_{j=1}^{m} \sum_{i=1}^{n} \frac{e_{ij}^2}{u_{ij}^2}, \quad (3)$$

where u_{ij} is an element of the uncertainty matrix (U), m is the number of species and n is the number of samples. A general optimization method where the measured value is 'weighted' by its uncertainty requires an accurate estimate of the uncertainty. The following 20 chemical species identified in elemental and ions analyses of the PM_{10} samples were used: S, K, Ti, Cr, Mn, Fe, Co, Cu, Zn, Br, Rb, Sr, Pb, Cl^-, NO_3^-, PO_4^{3-}, NH_4^+, Na^+, Mg^{2+} and Ca^{2+}. All of these data were classified as 'strong', which resulted in a high signal-to-noise ratio. In the present work, if the concentration is less than or equal to the detection limit (LOD) for a given element, the uncertainty is set at 5/6 LOD and the concentration replaced by 1/2 LOD [26,39]. The missing data were substituted by median values, and the corresponding uncertainties were set at four times the LOD median value [26,39]. After the factorization run, the PMF software provides the possibility of analyzing the factorization stability by the "Fpeak Bootstrap Method" [40]. Modeling was carried out together for the data from 2018 and 2020 years. The following values were obtained for Q robust 18,274; Q true 64,574.

2.6. Statistical Analysis

The Wilcoxon rank sum test was used to test whether there were significant differences in medians for solid fuel combustion, SIA, traffic/industry/construction work, soil contributions in both years 2018 and 2020. A value of 1 indicates a rejection of the statement that medians are equal; 0 indicates a failure to reject the statement that medians are equal. The Wilcoxon rank sum test is a nonparametric test that requires no specific distribution

on the measurements (like a normal distribution, for instance). This analysis tests the null hypothesis that the data in x and y are samples from continuous distributions with equal medians, against the alternative that they are not, where x and y are samples from 2018 and 2020. The result h = 1 indicates a rejection of the null hypothesis and h = 0 indicates a failure to reject the null hypothesis at the 5% significance level.

3. Results and Discussion

3.1. Chemical Analysis

Figure 3 shows the daily PM_{10} mass concentrations at the traffic-dominated station during the two sampling periods. Table 1 presents the minimum, maximum, and mean ± SD of the PM_{10} and element and ion concentrations at the traffic-dominated station in 2018 and 2020. It also presents a ratio of the concentrations in 2018 to the concentrations in 2020. Table S1 includes monthly concentrations of the PM_{10} and element and ion concentrations at a traffic-dominated station in 2018 and 2020. The PM_{10} decreased from 74 ± 29 $\mu g/m^3$ to 37 ± 13 $\mu g/m^3$ at the traffic station in 2018 and 2020, respectively. It was lowered by 61%, 54%, 34%, and 42% in February, March, April, and May in 2020 compared to 2018, respectively (Table S2). Table S2 shows the concentration of PM_{10} before the COVID-19 pandemic (in 2018 and 2017–2019) and during the pandemic (2020) in different cities. Filonchyk et al. observed a slightly lower drop in the PM_{10} concentrations than those observed by Filonchyk et al. for Krakow in the same period [32]. The PM_{10} lowering in February can be caused primarily by one reason. It is the introduction of a ban on the use of coal and wood for residential heating purposes in Krakow in September 2019. In March, two reasons can be observed. One is the introduction of the ban, and the second is the COVID-19 pandemic which started in March 2020 in Europe. In April and May, the differences between 2018 and 2020 were around 30–40%. It may be related to the limited activity of people during the COVID-19 pandemic, and especially the limited transport in Krakow. Filonchyk et al. observed smaller differences in the PM_{10} between 2018 and 2020 in March, April, and May in other Polish cities, namely Warszawa, Wrocław, Łódź, and Gdańsk [32]. Sicard et al. obtained a 51% and 48.7% reduction of the PM_{10} in the Valencia traffic station and Wuhan in March and April, respectively [41]. Strong differences in the concentration were observed for Cl. The 2018/2020 ratio was equal to 3.9. Its concentration decreased by 80%, 82%, and 20% in February, March, and May, respectively, while in April it increased by 31%. This element is an indicator of solid fuel combustion and the de-icing of roads in winter. Therefore, it can be expected that the emission related to solid fuel combustion will be lowered by a similar factor for 2020 compared to 2018. The concentrations of Cu, Zn, Ca, and Fe were lowered by 30–40% in April and May 2020. These elements are indicators of traffic. It could be caused by restrictions in activity during the COVID-19 pandemic. The concentration of K and Na^+ in 2018 was 2.3 times higher than in 2020. The NH_4^+ concentration was 2.5 times lower in 2020 than in 2018. K is an indicator of biomass burning, and NH_4^+ is a tracer of coal combustion, while Na^+ is connected to road dust and soil or salt. The following chemical species had similar concentrations at the station in both years: Ca, Ti, Mn, Ni, Rb, Sr, PO_4^{3-}, Mg^{2+}, K^+, and Ca^{2+}. The 2018/2020 ratio was in the range 0.9–1.2 for the species mentioned above. The ratio varying between 1.5 and 1.9 was for S, NO_3^-, SO_4^{2-}, Br, and Zn. The ratio for Fe, Co, and Cu was found to be equal to 1.4. The Cr concentration was higher in 2020 than in 2018. This element can come from the steel industry.

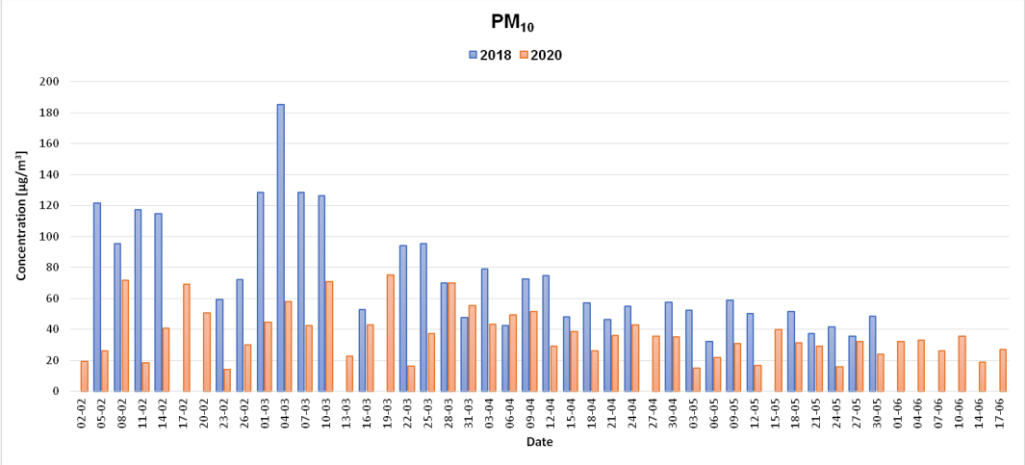

Figure 3. Daily PM_{10} concentration in measured periods 2018 and 2020 at the Krasińskiego traffic station in Krakow.

Table 1. The concentrations of PM_{10} (in $\mu g/m^3$) and their associated chemical species (in ng/m^3) in the year 2018 and 2020. One column contains the ratio of concentration in 2018 to concentration in 2020. The last column contains limit of detection (LOD—in ng/m^3).

Chemical Species	2018			2020			Ratio 2018/2020	LOD
	Min	Max	Mean ± SD	Min	Max	Mean ± SD		
PM_{10}	32	185	74 ± 29	14	75	37 ± 13	2.0	
S	48	2900	706 ± 400	126	945	400 ± 170	1.8	56
Cl	52	8450	1690 ± 1800	40	1330	433 ± 290	3.9	38
K	50	740	233 ± 95	11	273	100 ± 58	2.3	3.75
Ca	154	1970	794 ± 420	190	1800	780 ± 340	1.0	3.77
Ti	22	126	52 ± 17	16	110	51 ± 17	1.0	5.22
V	2.5	6.6	4.4 ± 1.3	<LOD	<LOD	<LOD		5.22
Cr	3.0	20	9.7 ± 3.8	8.1	49	31 ± 9	0.3	2.29
Mn	6.2	47	22.5 ± 7.3	5.1	45	20 ± 7	1.2	1.76
Fe	758	3164	1710 ± 470	386	2860	1340 ± 400	1.4	1.90
Co	3.4	18	10 ± 4	2.8	13	7.2 ± 2.1	1.4	1.74
Ni	1.4	4.1	2.5 ± 0.6	1.8	4.1	2.4 ± 0.5	1.1	0.04
Cu	20	80	45 ± 13	10	82	33 ± 11	1.4	1.46
Zn	20	433	114 ± 55	14	134	67 ± 23	1.7	1.42
As	0.9	6.4	2.4 ± 0.9	<LOD	<LOD	<LOD		
Br	1.1	38	8.5 ± 6.5	1.5	12	5 ± 3	1.7	1.13
Rb	0.5	2.7	1.2 ± 0.6	0.8	2.5	1.3 ± 0.5	0.9	0.36
Sr	1.4	12	3.9 ± 2.0	1.3	11	4.0 ± 1.7	1.0	0.29
Pb	2.8	48	15 ± 10	<LOD	<LOD	<LOD		5.37
NO_3^-	600	1570	4060 ± 2500	720	7620	2670 ± 1500	1.5	40
PO_4^{3-}	150	1940	540 ± 240	230	1060	560 ± 160	1.0	80
SO_4^{2-}	920	18,000	4500 ± 2500	960	4800	2400 ± 750	1.9	20
Na^+	440	11,000	2220 ± 1800	410	2660	960 ± 360	2.3	90
NH_4^+	120	7510	1150 ± 970	26	1800	460 ± 290	2.5	70
K^+	<LOD	1760	990 ± 210	240	1150	810 ± 80	1.2	47
Mg^{2+}	110	440	210 ± 60	110	290	170 ± 40	1.2	90
Ca^{2+}	1260	4200	2450 ± 580	1080	4000	2000 ± 500	1.2	90

SD—standard deviation, the variability of concentration during the measured period. LOD—limit of detection.

3.2. Preliminary Identification of PM_{10} Sources: An Element Enrichment Factor

Figure 4 shows the enrichment factors in decreasing order for the elements analyzed at the traffic-dominated station of Aleje Krasińskiego. The EFs were about 200 for Cl and Br and around 100 for Zn and Cu. They were in the range 50–10 for S, Pb, Co, As, and Cr (in

the year 2020). For example, Cl, Br, Zn, Pb, and As are released by coal combustion, Pb and Zn are caused by industrial processes and/or vehicle exhaust emissions, and Zn is caused by non-emissions (tire wear) [14,29]. Cu originates mainly from exhaust emissions (breast wear). Cr can come from coal burning, industry, or traffic [29]. Also, Cr can have a natural origin. For enrichment factors below 10, Cr (2018), Fe, Ni, V, Mn, K, Ca, Rb, and Sr are mainly of natural origin. These elements come not only from natural sources, but also from human emissions, which contribute to the PM_{10}. Ca can be associated with construction. Mn is associated with emissions from fuel additives or industrial processes. K is a marker for biomass combustion [14].

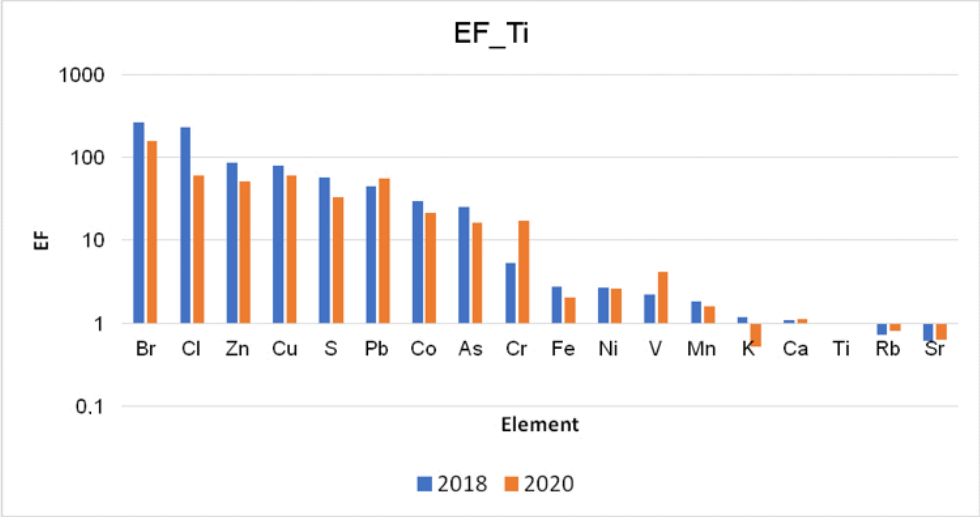

Figure 4. Enrichment factors for elements at Aleja Krasińskiego traffic-dominated station.

3.3. Source Apportionment PMF

Four factors were obtained from the PMF analysis. Figure 5 shows the factor profiles and attributed emission sources.

The first factor was characterized by Cl^- (81% of the mass), NO_3^- (27% of the mass), K (19% of the mass), Na^+ (16% of the mass). It was attributed to solid fuel combustion and the de-icing of roads in winter. Cl, S, Cd, Cr, and Br come from coal combustion [42,43]. K and Cl^- are the major compounds emitted from wood, straw, and other agricultural residues burning and are related to biomass burning [14,23,42,44]. The contribution of this source to the mass of the PM_{10} was equal to 15 $\mu g/m^3$ and 2.9 $\mu g/m^3$ in 2018 and 2020, respectively. The contribution decreased by 82% in 2020 compared to 2018. The most important lowering of this emission source contribution to the PM_{10} mass was observed in February and March. In these months, people heat their houses. This may be related to the introduction of the ban on the use of coal and wood for heating purposes in September 2019 in Krakow. The difference in the contribution to solid fuel combustion in 2018 and 2020 was very small in April and May (between 0.2 and 6.3 $\mu g/m^3$) when higher ambient temperatures were observed.

The second factor was attributed to secondary inorganic aerosols (SIAs) and the main chemical species were NH_4^+ (84% of the mass), S (33% of the mass), NO_3^- (27% of the mass), Br (31% of the mass), Pb (24% of the mass), and Co (17% of the mass). The SIA contribution was reduced from 15.5 $\mu g/m^3$ in 2018 to 2.3 $\mu g/m^3$ in 2020. It was reduced by around 84% during the entire analyzed period. In February and March, it decreased by 98% and 72%, respectively. In April it lowered by 35% and in May it increased by 90%. But the contribution of SIAs in April and May was very low and was in the range of 1.4–3.0 $\mu g/m^3$. SIAs are produced in the atmosphere by chemical reactions involving SO_2, NO_x, and NH_3. $(NH_4)2SO_4$ and NH_4NO_3 were the dominant components of SIAs in PM_{10}, which could be chemically formed by atmospheric reactions of NH_3 with SO_2 and NO_x emitted from high-temperature combustion processes using sulfur-containing fuels such as coal and

heavy fuel oil. The SO_4^{2-}/NO_3^- ratio was in the range 0.35–7.74 and 0.35–4.60 in 2018 and 2020, respectively. A higher ratio was observed for 2018 than for 2020. In particular, the main sources of SO_2 and NOx were coal-fired power plants, industrial boilers, and vehicular exhaust. The lowering of the above-mentioned ratio in 2020 can be connected to the lowering of the contribution of coal combustion. All elements included in this source are of dominantly or at least partly anthropogenic origin, as was confirmed by the analysis of the enrichment factors (Section 3.2.)

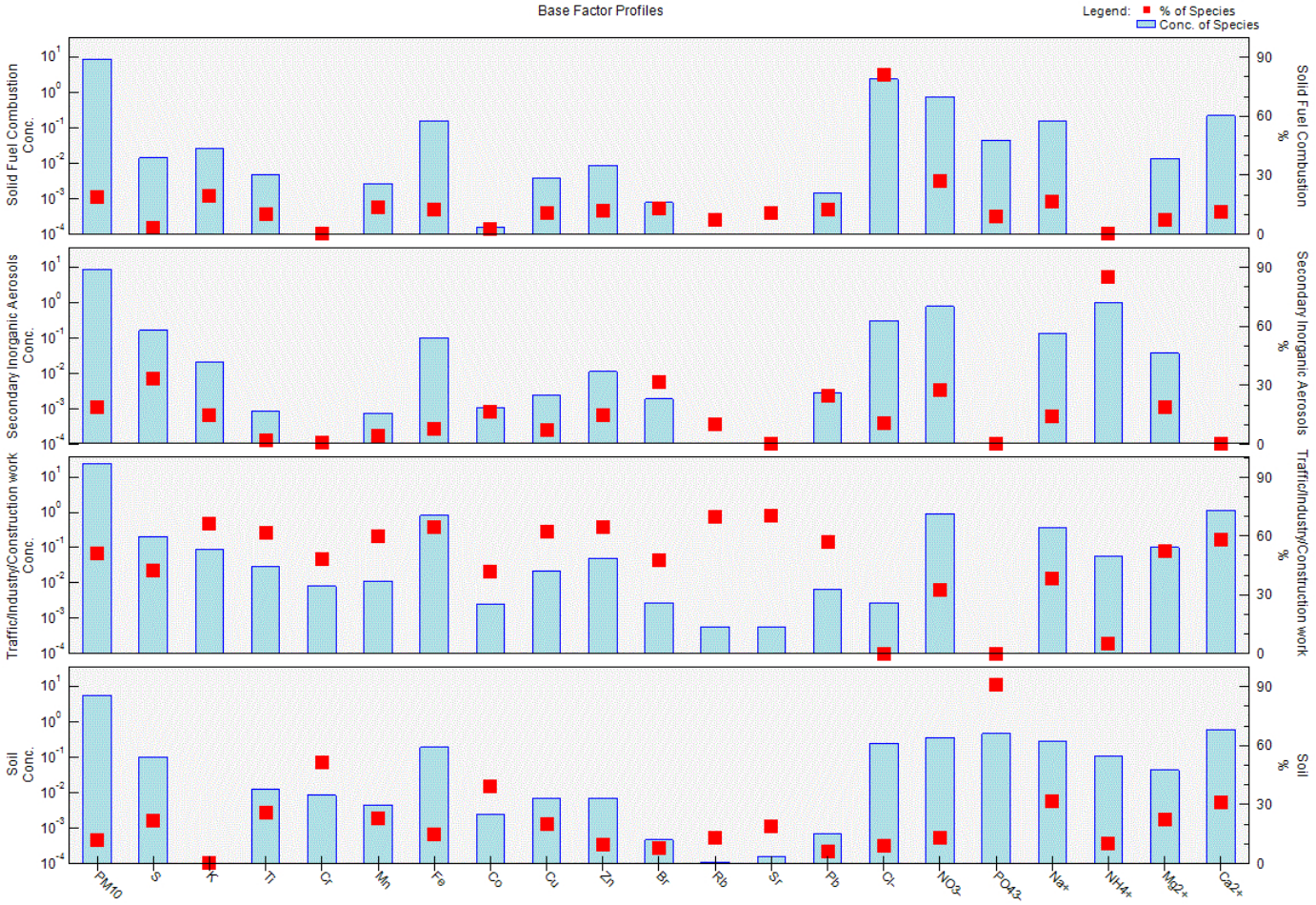

Figure 5. Factor profiles and attributed emission sources of PM_{10}.

The third factor characterized by Sr (70% of the mass), Rb (70% of the mass), Zn (66% of the mass), Fe (65% of the mass), K (67% of the mass), Ca^{2+} (58% of the mass), Cu (62% of the mass), Mn (60% of the mass), Ti (62% of the mass), S (42% of the mass), Na^+ (39% of the mass), Pb (58% of the mass), and Br (48% of the mass) was attributed to traffic/industry/construction work. Ti, Mn, Sr, Zr, Al, Ca, and Fe come from the resuspension of road dust [45,46]. Zn, Cu, Ba, Sb, and Fe are related to the wearing of brakes and tires [46–48]. Ti, Sr, and Fe may be emitted from the abrasion of roads, Fe, Mn, and Co from brake pads and Mn, Fe, and Co from tires [14] The contribution of this source to the PM10 mass was equal to 23.7 $\mu g/m^3$ and 23.1 $\mu g/m^3$ in 2018 and 2020 during the entire analysis period, respectively. In February, the contribution of this source was increasing by 30%, and in April it was on the same level in both analyzed years. In March and May, it was lowering by 6 and 36%, respectively. The decrease in emission source contribution could be caused by the reduction in activity during the COVID-19 pandemic which started in March 2020. It could also be the result of limited traffic in April and May 2020 during the COVID-19 pandemic.

The fourth factor was attributed to soil. The markers were PO_4^{3-} (92% of the mass), Cr (52% of the mass), Co (42% of the mass), Na^+ (31% of the mass), Ca^{2+} (31% of the mass), Mg^{2+} (22% of the mass), Cu (20% of the mass), Mn (23% of the mass), and Ti (26% of the mass). The contributions to the PM_{10} mass were 4.5 $\mu g/m^3$ and 6.5 $\mu g/m^3$ in 2018 and 2020, respectively. Non-identified sources contributed 14.5 $\mu g/m^3$ and 2.9$\mu g/m^3$ to the PM_{10} in 2018 and 2020, respectively. Figure 6 shows the factor fingerprints. Figure 7 presents the monthly contribution of sources to the mass of PM_{10} in $\mu g/m^3$.

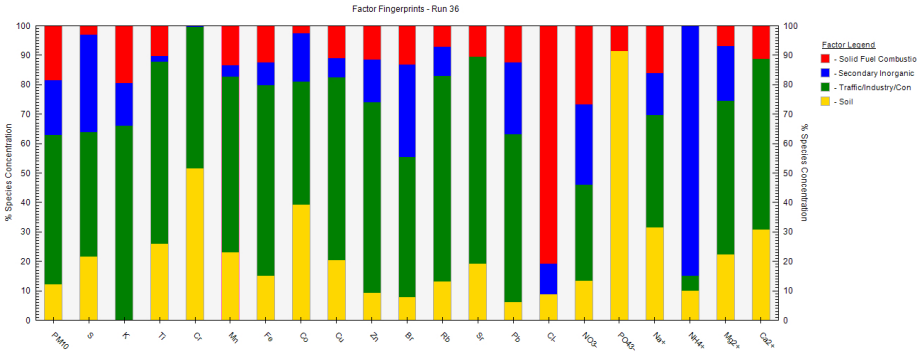

Figure 6. Factor fingerprints.

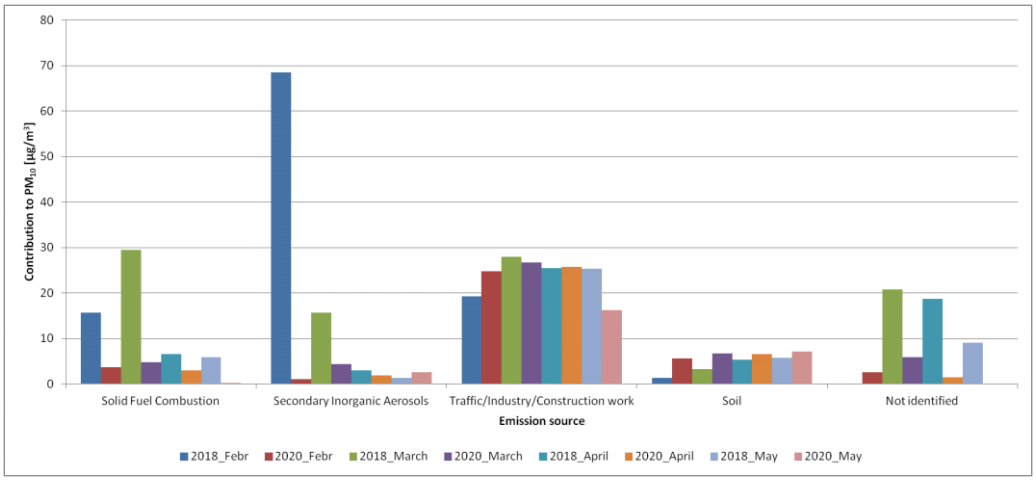

Figure 7. The monthly contribution of emission sources to PM_{10} at traffic-dominated station in Krakow in measured period 2018 and 2020.

For our DISP (displacement analysis), the results present no swaps that means the solution is stable. For our BS (bootstrapping analysis) analysis, the resulting mapping values met the criterion values (according to the PMF guideline document) for which it can be concluded that the number of factors is appropriate.

Gianini et al. [49] estimated that about 30% of the PM_{10} mass at the urban roadside site is generated by local road traffic emissions in Bern, Switzerland. Mineral matter (43%), secondary inorganic aerosol (SIA) (17%), organic matter and elemental carbon (31%) contribute to the PM10 mass in the urban location of Granada, Spain [50]. Dongarra et al. in Palermo, Italy, found that road traffic contributed almost 50% of the PM [51]. Road traffic, specifically emissions from vehicles, the suspension of dust due to vehicular movement, and tire break wear, add significantly to the PM_{10} around traffic sites [51–54].

Figure 8 presents the comparison of the modelled PM_{10} and measured PM_{10}. Figure S2 shows the predicted versus the observed concentration of chemical species.

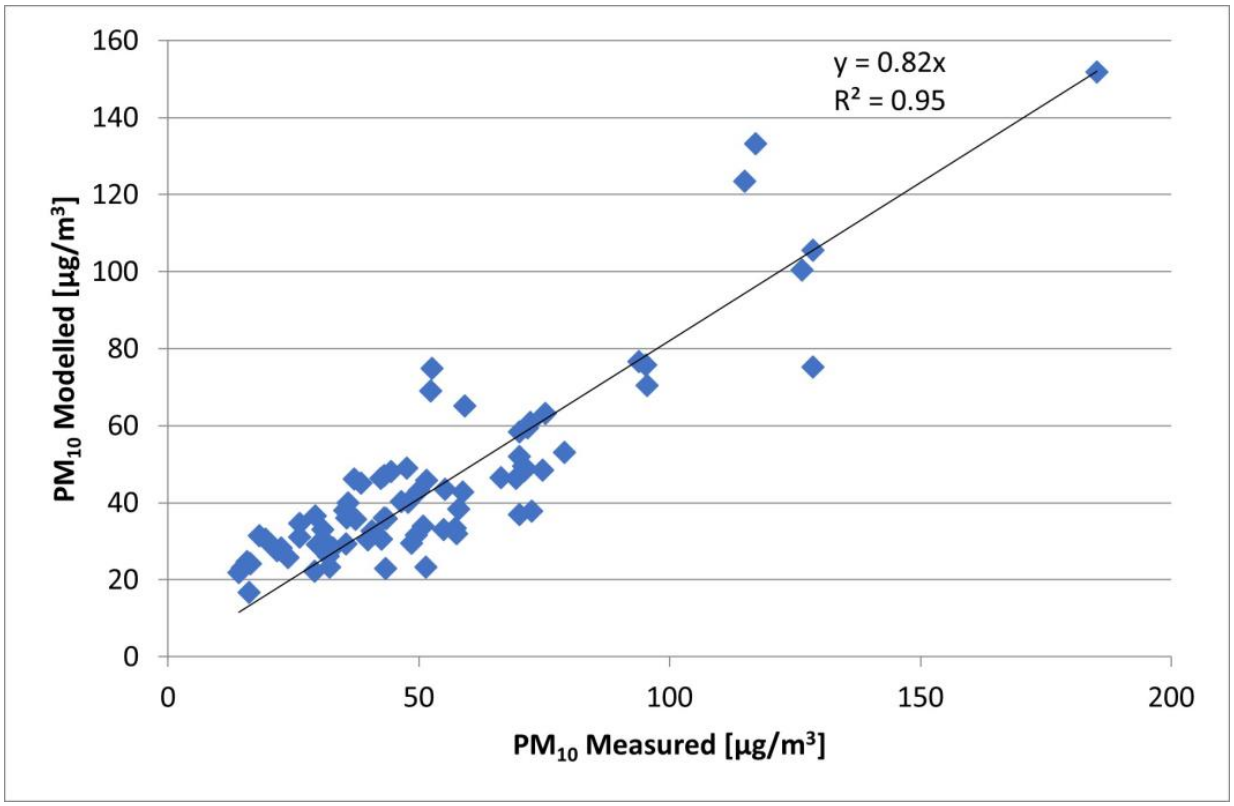

Figure 8. The comparison of modeled and measured PM_{10}.

Table 2 presents the results of the sources of contribution to the PM in the different urban areas.

Table 2. The contribution of different sources to PM mass in urban areas (in %).

Source	Poznań 2016/17 $PM_{2.5}$ [55]		Warszawa 2016, $PM_{2.5}$ [14]	Kraków, 2018/2019, $PM_{2.5}$ [29]	Kraków 2018/2019, PM_{10} [30]		Kraków, PM_{10} Present Study		Vienna 2006, PM10 [56]	Antwerp 1986, PM10 [56]	Lisbon 2006, PM10 [56]	Bamako (Mali) 2009 [57]	Dakar (Senegal) 2009 [57]
	Winter	Summer	Annual	Annual	Winter	Summer	2018 Spring	2020 Spring	Annual	Annual	Annual	Winter	Winter
Solid fuel combustion	36–55	7–9	45	43	10	nd	20	8				12	
SIA	28–45	28–45		24	28	5	21	7				16	
Traffic exhaust			21		24	48			50.7	21		47	49
Traffic	8–12	45–53	10										
Industry			11	28	24	32	33	64		16.5	19.7		10
Construction work			12										
Soil					7	9	6	18	16		18	30	25
Sea Salt										47	29.9		20
Other							20	4	33.3	19.5	34.4		

nd—not determined.

3.4. Statistical Analysis

The Wilcoxon rank sum test (Table 3) showed that significant statistical differences in solid fuel combustion were observed in March and May, and the SIA contributions were statistically different in February and March. The traffic/industry/construction work contributions were statistically different in May, falling by 36% in 2020 compared to 2018. It may be the result of the reduction in people's activity and traffic during the COVID-19 pandemic.

Table 3. Wilcoxon rank sum test results for solid fuel combustion, SIA, traffic/industry/construction work, and soil in both years 2018 and 2020. A value of 1 indicates a rejection of the statement that medians are equal; 0 indicates a failure to reject the statement that medians are equal.

	Solid Fuel Combustion	Secondary Inorganic Aerosols	Traffic/Industry/Construction Work	Soil
February	0	1	0	1
March	1	1	0	1
April	0	0	0	0
May	1	0	1	0

4. Conclusions

In this study, the effect of the lockdown on the air quality was assessed in Krakow. The PM10 concentrations at the Krakow traffic monitoring station decreased by 61%, 54%, 34%, and 42% in February, March, April, and May 2020 compared to the same months in 2018. The following elements and ions: Ca, Ti, Mn, Ni, Rb, Sr, PO_4^{3-}, Mg^{2+}, K^+, and Ca^{2+}, had similar concentrations in both years (2018 and 2020). The PMF modelling showed that the contributions of solid fuel combustion and SIA decreased by 77–84% and 98–72% in two months (February and March), respectively. The changes in the contribution of the sources in February 2020 could be caused by the introduction of a ban of the use of solid fuel combustion for residential heating in Krakow in September 2019. The high contribution of traffic/industry/construction work to the PM_{10} mass was equal to 24.6 $\mu g/m^3$ (33.1%) and 23.4 $\mu g/m^3$ (63.7%) in 2018 and 2020, respectively. In March and May 2020, it was reduced by 6% and 36%, respectively, compared to 2018. This may be related to the limited activity of people during the COVID-19 pandemic, especially the restriction of traffic in the city. In March 2020, the lockdown caused by the COVID-19 pandemic began.

Supplementary Materials: The following supporting information can be downloaded at: https://www.mdpi.com/article/10.3390/app132011492/s1.

Author Contributions: Conceptualization, L.S.; formal analysis, XRF L.S., J.D. and A.R.; IC analysis, K.S.; PMF modelling, Z.S.; funding acquisition, L.S., V.M. and S.M.A.; investigation, L.S.; methodology, L.S., K.S., A.R, J.D., V.M. and S.M.A.; project administration, L.S.; software, Z.S.; supervision, L.S.; validation, L.S., A.R., K.S. and Z.S.; roles/writing—original draft, L.S.; writing—review and editing, all. All authors have read and agreed to the published version of the manuscript.

Funding: The bilateral cooperation project (no BPN/BPT/2021/1/00001 in Poland and no 2021.09406. CBM in Portugal) between Poland and Portugal partially financed this work.

Institutional Review Board Statement: Not applicable.

Informed Consent Statement: Not applicable.

Data Availability Statement: The data are available on request from the authors.

Acknowledgments: This research project was supported/partially supported by the program 'Excellence initiative, research university' for the University of Science and Technology (Project no 1644). The bilateral cooperation project (no BPN/BPT/2021/1/00001 in Poland and no 2021.09406.CBM in Portugal) between Poland and Portugal partially financed this work together with the subsidy of the Ministry of Science and Higher Education, grants numbers 16.16.220.842 and 16.16.210.476. The authors thank the Voivodeship Inspectorate for Environmental Protection and the Chief Inspectorate of Environmental Protection for supplying the PM_{10} samples.

Conflicts of Interest: The authors declare no conflict of interest.

References

1. European Parliament; Council of the European Union. Directive 2008/50/EC of the European Parliament and the Council of 21 May 2008 on ambient air quality and cleaner air for Europe. *Off. J. Eur. Union* **2008**, *51*, 1–361.

2. GIOS. The Annual Reports of Air Quality Measurements of Chief Inspectorate of Environmental Protection, 2010–2019. Available online: https://powietrze.gios.gov.pl/ (accessed on 1 June 2021). (In Polish)
3. WIOS. The Annual Reports of Air Quality Measurements of Voivodeship Inspectorate for Environmental Protection in Krakow, 2010–2020. Available online: https://krakow.wios.gov.pl/ (accessed on 1 June 2021). (In Polish)
4. Alastuey, A.; Querol, X.; Plana, F.; Viana, M.; Ruiz, C.R.; Sánchez de la Campa, A.; de la Rosa, J.; Mantilla, E.; García dos Santos, S. Identification and Chemical Characterization of Industrial Particulate Matter Sources in Southwest Spain. *J. Air Waste Manag. Assoc.* **2006**, *56*, 993–1006. [CrossRef]
5. Belarbi, N.; Belamri, M.; Dahmani, B.; Benamar, M.A. Road Traffic and PM10, PM2.5 Emission at an Urban Area in Algeria: Identification and Statistical Analysis. *Pollution* **2020**, *6*, 651–660. [CrossRef]
6. Summak, G.; Ozdemir, H.; Oruc, I.; Kuzu, L.; Saral, A.; Demir, G. Statistical evaluation and predicting the possible sources of particulate matter in a Mediterranean metropolitan city. *Glob. NEST J.* **2018**, *20*, 173–180.
7. Mukherjee, A.; Agrawal, M. World air particulate matter: Sources, distribution and health effects. *Environ. Chem. Lett.* **2017**, *15*, 283–309. [CrossRef]
8. Sochacka-Tatara, E.; Majewska, R.; Perera, F.P.; Camann, D.; Spengler, J.; Wheelock, K.; Sowa, A.; Jacek, R.; Mróz, E.; Pac, A. Urinary polycyclic aromatic hydrocarbon metabolites among 3-year-old children from Krakow, Poland. *Environ. Res.* **2018**, *164*, 212–220. [CrossRef] [PubMed]
9. Konduracka, E.; Krawczyk, K.; Surmiak, M.; Pudełek, M.; Malinowski, K.P.; Mastalerz, L.; Zimnoch, M.; Samek, L.; Styszko, K.; Furman, L.; et al. Monocyte exposure to fine particulate matter results in miRNA release: A link between air pollution and potential clinical complication. *Environ. Toxicol. Pharmacol.* **2022**, *96*, 103996. Available online: https://www.sciencedirect.com/science/article/pii/S1382668922001892/pdfft?md5=323e7d3f525e618b2c26d3b26cdc5f6f&pid=1-s2.0-S1382668922001892-main.pdf (accessed on 17 October 2023). [CrossRef] [PubMed]
10. Reizer, M.; Juda-Rezler, K. Explaining the high PM10 concentrations observed in Polish urban areas. *Air Qual. Atmos. Health* **2016**, *9*, 517–531. [CrossRef] [PubMed]
11. Cohen, A.J.; Brauer, M.; Burnett, R.; Anderson, H.R.; Frostad, J.; Estep, K.; Balakrishnan, K.; Brunekreef, B.; Dandona, L.; Dandona, R.; et al. Estimates and 25-year trends of the global burden of disease attributable to ambient air pollution: An analysis of data from the Global Burden of Diseases Study 2015. *Lancet* **2017**, *389*, 1907–1918. [CrossRef] [PubMed]
12. Pope III, C.A.; Burnett, R.T.; Thun, M.J.; Calle, E.E.; Krewski, D.; Ito, K.; Thurston, G.D. Lung cancer, cardiopulmonary mortality, and long-term exposure to fine particulate air pollution. *JAMA* **2002**, *287*, 1132–1141. [CrossRef]
13. Pope, C.A., III; Ezzati, M.; Dockery, D.W. Fine-Particulate Air Pollution and Life Expectancy in the United States. *N. Engl. J. Med.* **2009**, *360*, 376–386. [CrossRef]
14. Juda-Rezler, K.; Reizer, M.; Maciejewska, K.; Błaszczak, B.; Klejnowski, K. Characterization of atmospheric PM2.5 sources at a Central European urban background site. *Sci. Total Environ.* **2020**, *713*, 136729. [CrossRef] [PubMed]
15. Belis, C.A.; Karagulian, F.; Larsen, B.R.; Hopke, P.K. Critical review and meta-analysis of ambient particulate matter source apportionment using receptor models in Europe. *Atmos. Environ.* **2013**, *69*, 94–108. [CrossRef]
16. Belis, C.A.; Larsen, B.R.; Amato, F.; El Haddad, I.; Favez, O.; Harrison, R.M.; Viana, M. European Guide on Air Pollution Source Apportionment with Receptor Models. 2014. Available online: https://www.researchgate.net/profile/Olivier-Favez/publication/335661273_European_guide_on_air_pollution_source_apportionment_with_receptor_models_-_Revised_version_2019/links/5f1d210045851515ef4a9f56/European-guide-on-air-pollution-source-apportionment-with-receptor-models-Revised-version-2019.pdf (accessed on 17 October 2023).
17. Belis, C.; Pernigotti, D.; Pirovano, G.; Favez, O.; Jaffrezo, J.; Kuenen, J.; van Der Gon, H.D.; Reizer, M.; Riffault, V.; Alleman, L.; et al. Evaluation of receptor and chemical transport models for PM10 source apportionment. *Atmos. Environ. X* **2019**, *5*, 100053. [CrossRef]
18. Hopke, P.K. Review of receptor modeling methods for source apportionment. *J. Air Waste Manag. Assoc.* **2016**, *66*, 237–259. [CrossRef] [PubMed]
19. Thunis, P.; Clappier, A.; Tarrasón, L.; Cuvelier, C.; Monteiro, A.; Pisoni, E.; Peduzzi, E. Source apportionment to support air quality planning: Strengths and weaknesses of existing approaches. *Environ. Int.* **2020**, *130*, 104825. [CrossRef] [PubMed]
20. Mircea, M.; Calori, G.; Pirovano, G.; Belis, C.A. European guide on air pollution source apportionment for particulate matter with source oriented models and their combined use with receptor models. *Publ. Off. Eur. Union Luxemb.* **2020**. [CrossRef]
21. Johnson, T.M.; Guttikunda, S.; Wells, G.J.; Artaxo, P.; Bond, T.C.; Russell, A.G.; Watson, J.G.; West, J. *Tools for Improving Air Quality Management: A Review of Top-Down Source Apportionment Techniques and Their Application in Developing Countries*; Report 339/11, Energy Sector Management Assistance Program; World Bank Group: Washington, DC, USA, 2011.
22. Kelly, F.J.; Fussell, J.C. Size, Source and Chemical Composition as Determinants of Toxicity Attributable to Ambient Particulate Matter. *Atmos. Environ.* **2012**, *60*, 504–526. [CrossRef]
23. Rys, A.; Samek, L.; Stegowski, Z.; Styszko, K. Comparison of concentrations of chemical species and emission sources PM2.5 before pandemic and during pandemic in Krakow, Poland. *Sci. Rep.* **2022**, *12*, 16481. [CrossRef]
24. Bokwa, A. *Wieloletnie Zmiany Struktury Mezoklimatu Miasta na Przykładzie Krakowa*; Instytut Geografii i Gospodarki Przestrzennej Uniwersytetu Jagiellońskiego: Kraków, Poland, 2010.
25. Bokwa, A. Rozwój badań nad klimatem lokalnym Krakowa. *Acta Geogr. Lodz.* **2019**, *108*, 7–20. [CrossRef]

26. Samek, L.; Stegowski, Z.; Furman, L.; Styszko, K.; Szramowiat, K.; Fiedor, J. Quantitative Assessment of PM2.5 Sources and Their Seasonal Variation in Krakow. *Water Air Soil Pollut.* **2017**, *228*, 290. [CrossRef]
27. Samek, L.; Stegowski, Z.; Styszko, K.; Furman, L.; Fiedor, J. Seasonal contribution of assessed sources to submicron and fine particulate matter in a Central European urban area. *Environ. Pollut.* **2018**, *241*, 406–411. [CrossRef] [PubMed]
28. Samek, L.; Stegowski, Z.; Styszko, K.; Furman, L.; Zimnoch, M.; Skiba, A.; Kistler, M.; Kasper-Giebl, A.; Rozanski, K.; Konduracka, E. Seasonal variations of chemical composition of PM2.5 fraction in the urban area of Krakow, Poland: PMF source attribution. *Air Qual. Atmos. Health* **2020**, *13*, 89–96. [CrossRef]
29. Samek, L.; Turek-Fijak, A.; Skiba, A.; Furman, P.; Styszko, K.; Furman, L.; Stegowski, Z. Complex characterization of fine fraction and source contribution to PM2.5 mass at an urban area in central Europe. *Atmosphere* **2020**, *11*, 1085. [CrossRef]
30. Samek, L.; Styszko, K.; Stegowski, Z.; Zimnoch, M.; Skiba, A.; Turek-Fijak, A.; Gorczyca, Z.; Furman, P.; Kasper-Giebl, A.; Rozanski, K. Comparison of PM_{10} Sources at Traffic and Urban Background Sites Based on Elemental, Chemical and Isotopic Composition: Case Study from Krakow, Southern Poland. *Atmosphere* **2021**, *12*, 1364. [CrossRef]
31. Casotto, R.; Skiba, A.; Rauber, M.; Strähl, J.; Tobler, A.; Bhattu, D.; Lamkaddam, H.; Manousakas, M.I.; Salazar, G.; Cui, T.; et al. Organic aerosol sources in Krakow, Poland, before implementation of a solid fuel residential heating ban. *Sci. Total Environ.* **2023**, *855*, 158655. [CrossRef] [PubMed]
32. Filonchyk, M.; Hurynovich, V.; Yan, H. Impact of Covid-19 lockdown on air quality in the Poland, Eastern Europe. *Sci. Total Environ.* **2020**, *198*, 110454. [CrossRef] [PubMed]
33. Collivignarelli, M.C.; Abbà, A.; Bertanza, G.; Pedrazzani, R.; Ricciardi, P.; Miino, M.C. Lockdown for COVID-2019 in Milan: What are the effects on air quality? *Sci. Total Environ.* **2020**, *732*, 139280. [CrossRef] [PubMed]
34. Polish Committee for Standardization. Atmospheric air—Standard gravimetric measurement method for determining the mass concentrations of PM10 or PM2.5 fractions of particulate matter. *PN EN* **2014**, *12*, 341.
35. Rudnick, R.L.; Gao, S. The composition of the continental crust. In *Treatise on Geochemistry—The Crust*; Rudnick, R.L., Holland, H.D., Turekian, K.K., Eds.; Elsevier: Oxford, UK, 2003; pp. 1–64.
36. Paatero, P.; Tapper, U. Positive matrix factorization: A Non-Negative Factor Model with Optimal Utilization of Error Estimates of Data Values. *Environmetrics* **1994**, *5*, 111–126. [CrossRef]
37. Karagulian, F.; Belis, C.A. Enhancing source apportionment with receptor models to foster the air quality directive implementation. *Int. J. Environ. Pollut.* **2012**, *50*, 190–199. [CrossRef]
38. Manousakas, M.; Diapouli, E.; Papaefthymiou, H.; Migliori, A.; Karydas, A.; Padilla-Alvarez, R.; Bogovac, M.; Kaiser, R.; Jaksic, M.; Bogdanovic-Radovic, I.; et al. Source apportionment by PMF on elemental concentrations obtained by PIXE analysis of PM10 samples collected at the vicinity of lignite power plants and mines in Megalopolis, Greece. *Nucl. Instrum. Methods Phys. Res. B* **2015**, *349*, 114–124. [CrossRef]
39. Polissar, A.V.; Hopke, P.K.; Paatero, P.; Malm, W.C.; Sisler, J.F. Atmospheric aerosol over Alaska: 2. Elemental composition and sources. *J. Geophys. Res. Atmos.* **1998**, *103*, 19045–19057. [CrossRef]
40. Manousakas, M.; Papaefthymiou, H.; Diapouli, E.; Migliori, A.; Karydas, A.; Bogdanovic-Radovic, I.; Eleftheriadis, K. Assessment of PM2.5 sources and their corresponding level of uncertainty in a coastal urban area using EPA PMF 5.0 enhanced diagnostics. *Sci. Total Environ.* **2017**, *574*, 155–164. [CrossRef] [PubMed]
41. Sicard, P.; De Marco, A.; Agathokleous, E.; Feng, Z.; Xu, X.; Paoletti, E.; Rodriguez, J.J.D.; Calatayud, V. Amplified ozone pollution in cities during the COVID-19 lockdown. *Sci. Total Environ.* **2020**, *735*, 139542. [CrossRef] [PubMed]
42. Yatkin, S.; Bayram, A. Elemental composition and sources of particulate matter in the ambient air of a Metropolitan City. *Atmos. Res.* **2007**, *85*, 126–139. [CrossRef]
43. Agarwal, A.; Satsangi, A.; Lakhani, A.; Kumari, K.M. Seasonal and spatial variability of secondary inorganic aerosols in PM2.5 at Agra: Source apportionment through receptor models. *Chemosphere* **2019**, *242*, 125132. [CrossRef] [PubMed]
44. Saarikoski, S.; Timonen, H.; Saarnio, K.; Aurela, M.; Järvi, L.; Keronen, P.; Kerminen, V.-M.; Hillamo, R. Sources of organic carbon in fine particulate matter in northern European urban air. *Atmos. Chem. Phys.* **2008**, *8*, 6281–6295. [CrossRef]
45. Sternbeck, J.; Sjödin, Å.; Andréasson, K. Metal emissions from road traffic and the influence of resuspension—Results from two tunnel studies. *Atmos. Environ.* **2002**, *36*, 4735–4744. [CrossRef]
46. Querol, X.; Viana, M.; Alastuey, A.; Amato, F.; Moreno, T.; Castillo, S.; Pey, J.; de la Rosa, J.; de la Campa, A.S.; Artíñano, B.; et al. Source origin of trace elements in PM from regional background, urban and industrial sites of Spain. *Atmos. Environ.* **2007**, *41*, 7219–7231. [CrossRef]
47. Hampel, R.; Peters, A.; Beelen, R.; Brunekreef, B.; Cyrys, J.; de Faire, U.; de Hoogh, K.; Fuks, K.; Hoffmann, B.; Hüls, A.; et al. Long-term effects of elemental composition of particulate matter on inflammatory blood markers in European cohorts. *Environ. Int.* **2015**, *82*, 76–84. [CrossRef]
48. Samek, L.; Gdowik, A.; Ogarek, J.; Furman, L. Elemental composition and rough source apportionment of fine particulate matter in air in Cracow, Poland. *Environ. Prot. Eng.* **2016**, *42*, 71–83. [CrossRef]
49. Gianini, M.F.; Gehrig, R.; Fischer, A.; Ulrich, A.; Wichser, A.; Hueglin, C. Chemical composition of PM10 in Switzerland: An analysis for 2008/2009 and changes since 1998/1999. *Atmos. Environ.* **2012**, *54*, 97–106. [CrossRef]
50. Titos, G.; Foyo-Moreno, I.; Lyamani, H.; Querol, X.; Alastuey, A.; Alados-Arboledas, L. Optical properties and chemical composition of aerosol particles at an urban location: An estimation of the aerosol mass scattering and absorption efficiencies. *J. Geophys. Res. Atmos.* **2012**, *117*, 1–12. [CrossRef]

51. Dongarrà, G.; Manno, E.; Varrica, D.; Lombardo, M.; Vultaggio, M. Study on ambient concentrations of PM10, PM10–2.5, PM2.5 and gaseous pollutants. Trace elements and chemical speciation of atmospheric particulates. *Atmos. Environ.* **2010**, *44*, 5244–5257. [CrossRef]
52. Mansha, M.; Ghauri, B.; Rahman, S.; Amman, A. Characterization and source apportionment of ambient air particulate matter (PM2.5) in Karachi. *Sci. Total Environ.* **2012**, *425*, 176–183. [CrossRef] [PubMed]
53. Tiwari, S.; Srivastava, A.K.; Bisht, D.S.; Bano, T.; Singh, S.; Behura, S.; Srivastava, M.K.; Chate, D.M.; Padmanabhamurty, B. Black carbon and chemical characteristics of PM10 and PM2.5 at an urban site of North India. *J. Atmos. Chem.* **2010**, *62*, 193–209. [CrossRef]
54. Rahman, S.A.; Hamzah, M.S.; Wood, A.K.; Elias, S.; Salim, N.A.A.; Sanuri, E. Sources apportionment of fine and coarse aerosol in Klang Valley, Kuala Lumpur using positive matrix factorization. *Atmos. Pollut. Res.* **2011**, *2*, 197–206. [CrossRef]
55. Chlebowska-Styś, A. Identyfikacja Źródeł Emisji Pyłu Zawieszonego na Terenie Poznania. Ph.D. Dissertation, Wydział Inżynierii Środowiska, Politechnika Wrocławska, Wrocław, Poland, 2020.
56. Database on Source Apportionment Studies for Particulate Matter. Available online: https://www.who.int/data/gho/data/themes/air-pollution/source-apportionment-db (accessed on 3 October 2023).
57. Doumbia, T.; Liousse, C.; Ouafo-Leumbe, M.-R.; Ndiaye, S.A.; Gardrat, E.; Galy-Lacaux, C.; Zouiten, C.; Yoboué, V.; Granier, C. Source Apportionment of Ambient Particulate Matter (PM) in Two Western African Urban Sites (Dakar in Senegal and Bamako in Mali). *Atmosphere* **2023**, *14*, 684. [CrossRef]